JOURNAL OF MASS SPECTROMETRY
J. Mass Spectrom. 2005; **40**: 899–907
Published online 2 June 2005 in Wiley InterScience (www.interscience.wiley.com). DOI: 10.1002/jms.866

JMS

Chromophore effect in photodissociation at 266 nm of protonated peptides generated by matrix-assisted laser desorption ionization (MALDI)

Joo Yeon Oh, Jeong Hee Moon and Myung Soo Kim*

National Creative Research Initiative Center for Control of Reaction Dynamics and School of Chemistry, Seoul National University, Seoul 151–742, Korea

Received 5 November 2004; Accepted 21 March 2005

Chromophore effect in the photodissociation of protonated peptides at 266 nm was investigated using synthetic peptides with the sequence RGGXGGGGGR where X was a phenylalanyl(F), tyrosyl(Y), cysteinyl(C), glycyl(G), seryl(S), or histidyl(H) residue. The peptides with an F or Y residue dissociated efficiently. Fragment ions due to cleavages at either end of the chromophore were especially prominent just as for the peptide with a tryptophanyl residue reported previously.[1] Photodissociation was observed even for the peptides without any noticeable chromophore at 266 nm. Here, dissociation at all the peptide bonds was almost equally prominent. Photodissociation of the protonated angiotensin I was investigated using the spectral correlation rules observed in the model systems. Role of the chromophores and the plausible mechanisms involved are discussed. Copyright © 2005 John Wiley & Sons, Ltd.

KEYWORDS: MS/MS; MALDI; photodissociation of peptides

INTRODUCTION

Tandem mass spectrometry combined with matrix-assisted laser desorption ionization(MALDI)[2–4] or with electrospray ionization (ESI)[5,6] has become one of the major tools for the structure determination of biomolecules. In tandem mass spectrometry,[7] various techniques are used to activate a precursor ion and thereby to induce its dissociation, collisional activation[8–11] being the most popular among these techniques.

Conceptually the most appropriate mass analyzer for MALDI, which is a pulsed ionization technique, is the time-of-flight (TOF) analyzer.[12] Commercial MALDI-TOF mass spectrometers equipped with a reflectron are widely available now. This type of instruments can readily detect fragment ions formed in the field-free region between the ion source and the reflection. The internal energy of a precursor ion acquired at the time of its formation or via collisional activation in the source is thought to be responsible for this post-source decay (PSD) process.[13,14] Installation of an ion gate to select the precursor ion of interest is the instrumental requirement for PSD tandem mass spectrometry.[14] Efforts are being made to design an ion gate that can select a monoisotopic precursor ion efficiently.[15,16] More troublesome than this technical difficulty is the fact that information available from a PSD spectrum is usually not sufficient for a definite structural analysis. Introducing a collision gas and thus inducing collisionally activated dissociation (CAD)[17] is an attempt to improve the information content of a tandem mass spectrum. A method to improve the resolution is needed for CAD in TOF, such as the use of a lift cell,[18,19] because a collision affects the quality of a precursor ion beam.

Photodissociation (PD) using a pulsed ultraviolet (UV) laser[20–26] has been attracting some attention as an alternative to CAD. The fact that introducing photons is compatible with the very high vacuum requirement for the analyzer and that the photoabsorption does not affect the beam quality have been mentioned as the apparent advantages of PD over CAD. Also, the possibility to select a monoisotopic precursor via laser-ion synchronization has been mentioned.

Recently, we built a tandem TOF mass spectrometer dedicated to photodissociation study of protonated peptides at 266 nm generated by a commercial Nd : YAG laser.[27] Our first concern was whether the output from a commercial laser would be adequate to induce fragmentation of a significant fraction of the precursor ions. For samples containing an aromatic residue, around 5 mJ of laser pulse focused cylindrically could deplete the precursor ion by around 50%. Almost complete depletion was possible as the pulse energy was further increased. Quality of the fragment ion spectra recorded was decent but not as good as the CAD spectra recorded by commercial instruments in resolution and sensitivity, probably due to various deficiencies of the homebuilt instrument such as in the MALDI source design and data system. However, the fact that the parent ion depletion by PD is comparable to that in

*Correspondence to: Myung Soo Kim, School of Chemistry, Seoul National University, Seoul 151–742, Korea.
E-mail: myungsoo@plaza.snu.ac.kr
Contract/grant sponsor: CRI, Ministry of Science and Technology, Republic of Korea.

JMS

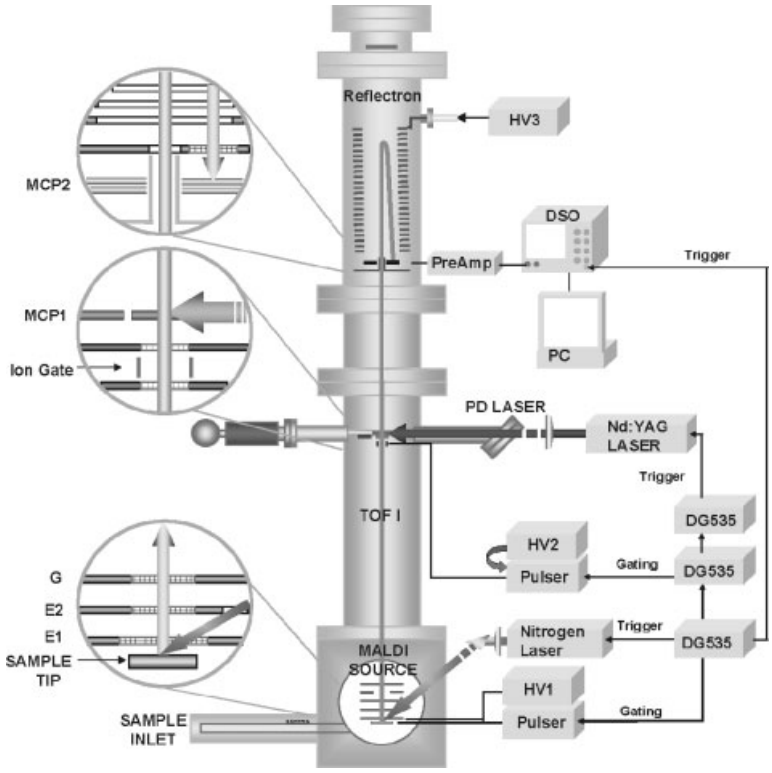

Figure 1. A schematic diagram of the MALDI-TOF-PD-TOF instrument used in this work.

CAD suggests comparable efficiencies of the two techniques. Also, monoisotopic selection of a precursor ion via laser-ion synchronization was demonstrated for the first time, with the precursor ion resolving power of around 2000.[27]

As mentioned earlier, CAD usually generates much more sequence-specific ions from protonated peptides than PSD. The same must be the case with PD for it to be useful as a structure probe, which was our next concern. A subsequent study with a synthetic peptide with a tryptophanyl residue showed PD fragments formed by cleavages at almost all the peptide bonds.[1] Also observed was that cleavages at either end of the tryptophanyl residue, the chromophore at 266 nm, were especially prominent indicating nonstatistical reactions occurring near this residue.

As a continuation of our effort to understand the role of UV chromophore in PD tandem mass spectrometry at 266 nm, the tryptophanyl residue in the original synthetic peptide was replaced by others and PD was attempted. To our surprise, PD was observed even for peptides without a noticeable UV chromophore, even though at much larger PD laser pulse energy. The results are reported in this paper.

EXPERIMENTAL

Details of the homebuilt MALDI-TOF-PD-TOF spectrometer (Fig. 1) were reported previously.[27] Briefly, the spectrometer consists of the MALDI source with delayed extraction, the first TOF analyzer that separated precursor ions in time-of-flight, and the second TOF analyzer that analyzes fragment ions. The first TOF is a linear type, while the second was a reflectron consisting of 24 coaxial electrode plates connected by resistors such that the potential inside the reflectron is linear-plus-quadratic (LPQ), or $V = c_1x + c_2x^2$ where x is the distance from the reflectron entrance. An ion gate consisting of two electrode plates parallel to the ion beam direction is installed immediately before the first time focus. The precursor ion selection is achieved by switching off the field inside the gate. Resolving power of the ion gate is around 30.

A pulsed nitrogen laser (VSL-337ND-S, Laser Science, Franklin, MA) with 300 μJ per pulse at 337.1 nm and <4 ns pulse width was used for MALDI. Its pulse energy was adjusted with a neutral density filter. The fourth harmonic, 266 nm, of an Nd : YAG laser(Surelite III-10, Continuum, Santa Clara, CA) with 5 ns pulse width was used as the PD laser, which was focused cylindrically at a position immediately after the ion gate.

The sample plate was switched from 13 to 14.4 kV some time after MALDI and the ion gate voltage 0.5 kV was switched off when the precursor ion of interest entered the gate. Tandem mass spectra were recorded with the final electrode of the reflectron at 17, 10, and 6 kV. Time sequence for the laser pulsing and electrode voltage switching was achieved by three delay generators (DG535, SRS, Sunnyvale, CA). Ion signal was detected by an MCP, preamplified, and recorded by a digital storage oscilloscope (LT372; Lecroy, Chesnut Ridge, NY). Spectra were recorded with and without the PD laser alternately and averaged for 10–25 PD laser shots and the results were transferred to a personal computer. A spectrum recorded without the PD laser consists of MALDI ions passing the ion gate and their PSD fragments. To record the laser-induced spectral change only, this was subtracted from the laser-on spectrum, resulting in the PD spectrum. Spectra averaged over 3000–5000 PD laser shots will be shown.

To compare with the PD spectra, CAD spectra for the protonated peptides were obtained also using a Q-TOF

instrument (API Qstar Pulsar i, Applied Biosystem, CA) equipped with an ESI source.

Angiotensin I and the matrix, α-cyano-4-hydroxycinnamic acid (CHCA), were purchased from Sigma(St. Louis, MO) and synthetic peptides from Peptron(Daejon, Korea). For MALDI experiments, matrix solution was prepared daily using acetonitrile and 0.1% trifluoroacetic acid. Sample solution was prepared by mixing peptide and matrix solutions. 1 μl droplet of the sample solution was loaded on the sample plate and air-dried. A relatively large amount of a peptide, around 100 pmol/μl, was routinely used for extensive PSD and PD studies. All the peptide samples for ESI-CAD experiments were prepared at the concentration of 10 pmol/μl. Acetic acid was added (0.1–0.4%) as needed.

RESULTS

In the previous study,[1] we carried out detailed fragmentation study of a synthetic peptide with a tryptophanyl residue, RGGWGGGGGR, where R, G, and W represent the arginyl, glycyl, and tryptophanyl residues, respectively. This was intentional because tryptophan was a good chromophore at 266 nm used for PD and therefore a peptide with tryptophan as a residue was expected to display efficient photodissociation. A synthetic peptide was chosen rather than more familiar prototype peptides because investigation of the influence of one chromophore at a time on photodissociation was desired. Arginine was attached at both ends of the peptide to facilitate observation of fragment ions with charge retention both in the C-terminus and in the N-terminus. Following the same strategy, photodissociation of the protonated synthetic peptides with the sequence RGGXGGGGGR where X is a phenylalanyl(F), tyrosyl(Y), cysteinyl(C), glycyl(G), seryl(S), or histidyl(H) residue has been investigated in this work. These will be called the peptide F, Y, C, G, S, and H, respectively. Tryptophan, phenylalanine, tyrosine, and cysteine are UV chromophores with the molar extinction coefficients at 253.7 nm of 2870, 140, 320, and 270, respectively, for 0.1 M HCl aqueous solutions.[28] Those for glycine, serine, and histidine are nearly insignificant, around 0.2. Information on the UV absorption of amino acids and peptides in the gas phase is hardly available. For the amino acids W, F, and Y, Levy and coworkers[29,30] and Lubman and coworkers[31,32] reported gas phase absorption occurring in the same spectral region as in the aqueous solution phase suggesting that the solution phase data can be a reasonable guide in this matter. Major sequence-specific fragment ions(sequence ions) from a protonated peptide are formed by cleavages at the peptide bonds. A rigorous nomenclature for sequence ions has been proposed,[33] its abbreviated form will be used here.

Amino acid residues are numbered starting from the left to differentiate a, b, and c fragment ions generated by cleavages at various peptide bonds and from the right for x, y, and z. Side chain loss may accompany peptide bond cleavages generating d, v, and w fragment ions.[13] v_n generated by a side chain loss from y_n is particularly important for the peptides W, F, Y, S and H. Internal acyl ions[12] generated by cleavages of two peptide bonds may be expressed such as XGG. Instead, the expression XG2 will be used because we can not distinguish GGX, GXG, and XGG.

Peptides with a chromophore at 266 nm

Before presenting the PD results for the peptides with a phenylalanyl, tyrosyl, or cysteinyl residue, let us first briefly summarize the features in PD of the protonated RGGWGGGGGR, or the peptide W, reported previously.[1] A variety of sequence ions were observed, namely, a_i (i = 3–9), b_3, c_3, x_i(i = 7,9), y_i(i = 1–6), and z_i(i = 2–7,9) together with v_7 and the neutral loss peaks a_i-NH_3(i = 3–9), and b_i-NH_3(i = 2,3) – cleavages at all the peptide bonds resulted in one or more sequence ions. Almost all the remaining prominent peaks could be assigned, mostly to the internal acyl ions such as G4, WG, WG2, and WG3. a_4, y_6, and v_7 were particularly intense, which were the fragments formed by cleavages at either end of the tryptophanyl residue. In PD of the protonated RGGGGGWGGR, a_7, a_7-NH_3, and c_6 were very intense, which were also the fragments formed by cleavages in the vicinity of W. It was suggested that the energy initially deposited in the tryptophanyl residue by photoabsorption do not flow very rapidly to other moieties, resulting in nonstatistical dissociations near this residue.

The PSD and PD spectra of the protonated peptide F are shown in Fig. 2. The PD spectrum was obtained with 7 mJ per pulse at 266 nm measured at the ion beam position, which resulted in 35% depletion of the lowest mass isotopic peak, or A peak, of MH^+. It is to be mentioned that 3 mJ laser pulse energy resulted in 45% depletion for the peptide W. Four peaks dominate the PSD spectrum of the peptide F, namely, those at 860.4, 859.5, 835.4, and 721.4, which can be assigned to $[MH\text{-}NH_3]^+$, $[MH\text{-}H_2O]^+$, $[MH\text{-}CH_2N_2]^+$, and y_9, respectively. Loss of CH_2N_2 occurred presumably at one of the arginyl residues. Other less intense peaks are the sequence ions a_4, b_9, y_5, and y_6. Among the peptide bonds, the one between G and R at the N-terminus must be the most labile because y_9 is the most intense among the sequence ions. The same was observed for the peptide W.

Compared to the PSD spectrum, the PD spectrum in Fig. 2 displays a far richer spectral pattern. Even so, most of the prominent peaks can be reasonably assigned as will be described below. Another striking feature of the PD spectrum is the monoisotopic nature of each peak, evident when y_9 peaks in the PD and PSD spectra are compared. Monoisotopic selection via laser-ion synchronization is one of the important characteristics of the present PD technique as explained earlier. Cleavages at all the peptide bonds resulted in one or more sequence ions as marked in the figure. These are a_i(i = 1–9), b_i(i = 4,5,9), c_i(i = 5), x_i(i = 3,6), y_i(i = 1–9), z_i(i = 1–6,9), a_i-NH_3(i = 1–6,8,9), b_i-NH_3(i = 1–6), and v_7. Some internal acyl ions also appear prominently, such as G3(172.4), G4(229.2), G5(286.1), and FG3(319.5). Compared to the other sequence ions, a_4-NH_3(373.4), a_4(390.4), y_6(460.3), v_7(515.2), y_7(607.2), y_8(664.2), a_9(675.3), b_9, or y_9-H_2O(703.5), z_9(704.3), and y_9(721.4) appear prominently in the PD spectrum. Among these, a_4-NH_3, a_4, y_6, v_7 and y_7 are due to cleavages at either end of F while a_9, b_9, z_9, and y_9 are due to cleavages in the first peptide bonds at the N- and C-termini. As will be seen, the latter group of fragments

JMS

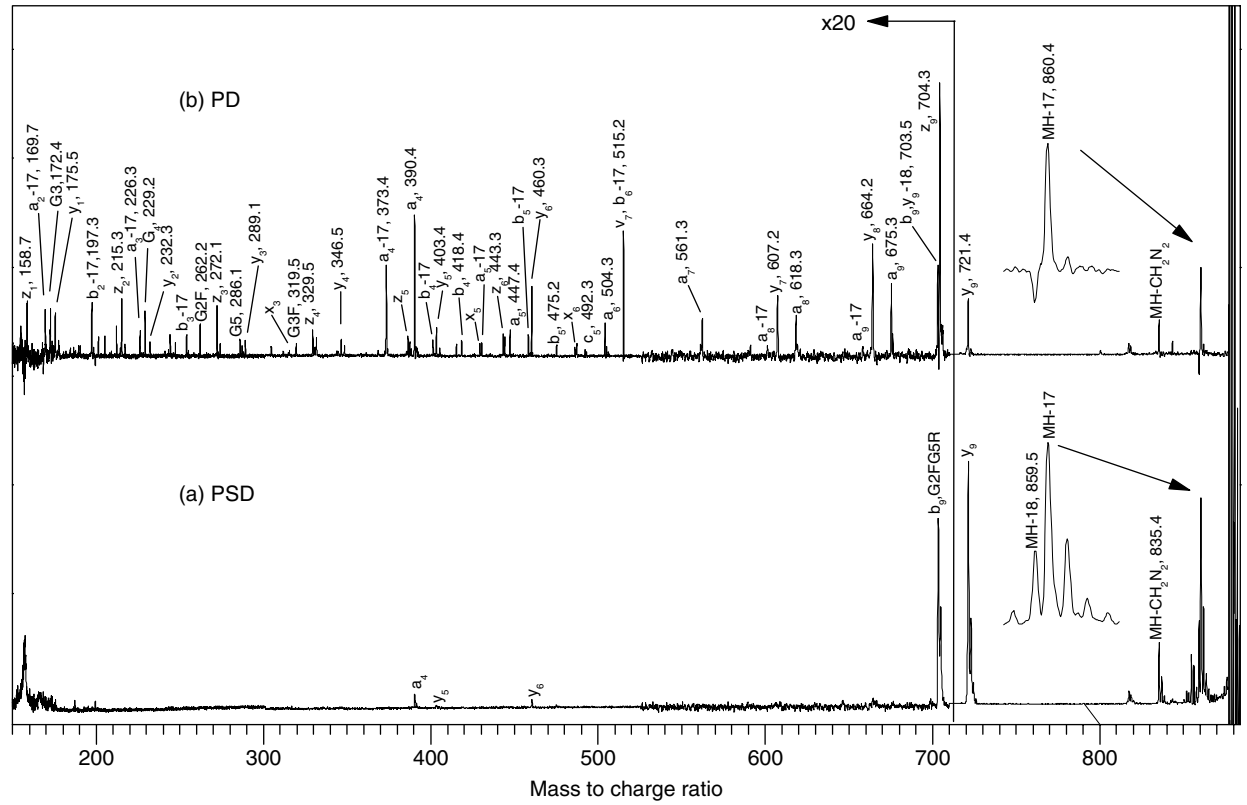

Figure 2. (a) PSD and (b) PD spectra of MH^+ generated by MALDI of the peptide F. The ion gate was set to transmit MH^+. 7 mJ PD laser pulse energy resulted in 35% depletion of MH^+. The PD spectrum was obtained by subtracting the PSD(laser-off) spectrum from the laser-on spectrum.

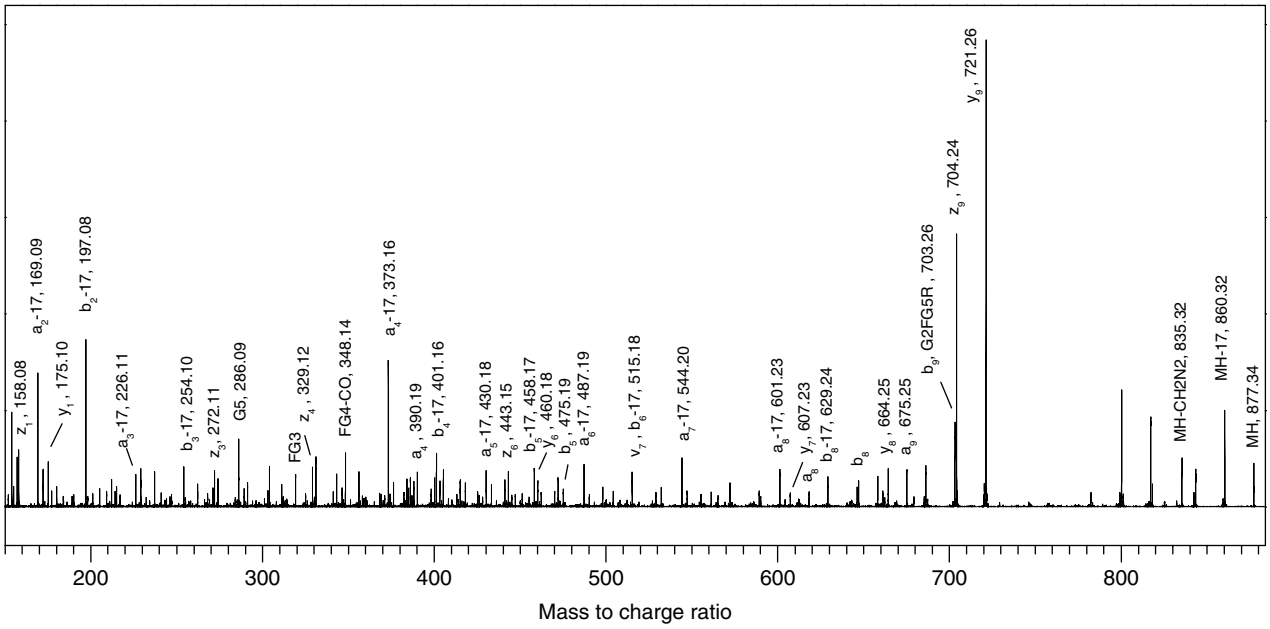

Figure 3. CAD spectrum of MH^+ generated by ESI of the peptide F.

appear prominently in the PD spectra of other protonated peptides also, indicating that facile cleavage of the terminal peptide bonds is one of the characteristics of RGGXGGGGGR synthesized. Then, prominence of a_4-NH_3, a_4, y_6, v_7, and y_7, which are due to cleavages at either end of F, suggests site-specific, or nonstatistical reactions at the hot spot generated by UV absorption.

To see if the prominence of the fragment ions generated at either end of F is characteristic of photodissociation, CAD spectra of the protonated peptide F generated by ESI were recorded with a Q-TOF instrument. A CAD spectrum obtained at around 90% attenuation of the parent ion intensity is shown in Fig. 3. In this spectrum, $[MH\text{-}NH_3]^+$, $[MH\text{-}CH_2N_2]^+$, y_9, z_9, and b_8 were very prominent

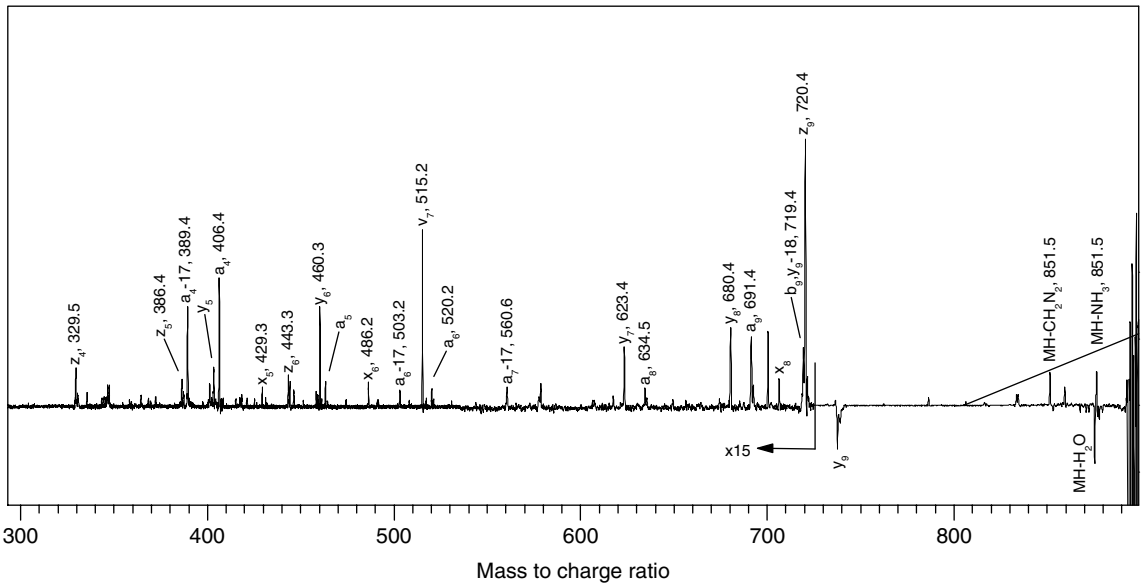

Figure 4. PD spectrum of MH^+ generated by MALDI of the peptide Y. 7 mJ PD laser pulse energy resulted in 50% depletion of MH^+.

as in the PSD and PD spectra, indicating that these are generated via low energy reaction channels and are not characteristic of the activation method used. At lower m/z than the above, most of the fragments observed in the PD spectrum find their counterparts in the CAD spectrum. However, the site-specific fragment ions mentioned above are not particularly prominent in the CAD spectrum except for a_4-17. For example, the a_4, y_6, and y_7 fragments are less than spectacular in CAD. CAD spectra recorded at various collision energies displayed similar patterns. We also recorded CAD spectra of the doubly protonated peptide F and of the singly and doubly protonated peptide W and Y. The results were similar: the fragments generated by cleavages near the terminus were very prominent and a_4-17 fragments were somewhat prominent. Low energy collisional activation is not a site-specific process. CAD occurring under such a condition is thought to be more or less statistical. Then, prominence of the fragments a_4, y_6, v_7, and y_7 observed in PD may indicate participation of nonstatistical processes as mentioned previously. In fact, both statistical and nonstatistical processes may contribute to generation of the whole PD spectrum.

The PD spectrum of the peptide Y is shown in Fig. 4. Around 7 mJ of the laser pulse energy resulted in around 50% depletion of the precursor ion intensity. The PSD spectrum of the peptide Y, and those of the other peptides will not be shown because they are virtually the same as that of the peptide F, dominated by $[MH\text{-}NH_3]^+$, $[MH\text{-}H_2O]^+$, $[MH\text{-}CH_2N_2]^+$, and y_9. In the PD spectrum, the sequence characteristic fragments y_8, a_9, b_9 or $y_9\text{-}H_2O$, and z_9 appear prominently at m/z680.4, 691.4, 719.4, and 720.4, respectively, even though y_9 appears as a negative peak due to efficient photodissociation of the same ion generated by PSD. Other than these, $a_4\text{-}NH_3$(389.4), a_4(406.4), y_6(460.3), and v_7(515.2) dominate the PD spectrum just as in the cases of the peptides W and F.

Strong photodissociation of the protonated peptide C at 266 nm was expected considering the significant molar extinction coefficient at 253.7 nm for the free cysteine in acidic aqueous solution.[28] Much higher PD laser power was needed against this expectation, 30 mJ pulse energy resulting in around 25% depletion. The PD spectrum thus obtained is shown in Fig. 5. Here again, y_8, a_9, and z_9 appear prominently and b_9 less prominently. y_9 appears as a negative peak as for the peptide Y. A remarkable feature of this spectrum compared with those for the peptides W, F and Y, however, is that $a_4\text{-}NH_3$(329.5), a_4(346.5), and y_6(460.3) are not particularly prominent compared to other sequence ions such as y_5(or a_5) at 403.5 and y_7 at 563.2. Rather, the spectrum consists of many sequence peaks with comparable intensities.

Peptides without a significant chromophore at 266 nm

Without a UV chromophore such as W, F, Y, and C, a protonated peptide is not expected to display strong absorption at 266 nm. However, strong PD was observed for such peptides even though at much larger laser pulse energy than used for the peptides with an aromatic residue.

The PD spectrum for the peptide G is shown in Fig. 6. 30 mJ laser pulse energy was used to record this spectrum, which resulted in around 10% depletion of the precursor ion. y_8(574.2), a_9(585.2), b_9 or $y_9\text{-}H_2O$(613.3), and z_9(614.2) appear distinctly as before. a_4 and y_6 are distinct, but are not particularly prominent compared to other sequence ions and a_4-17 is hardly observable unlike the cases with an aromatic residue. Rather, the spectrum consists mostly of the sequence and internal acyl peaks, with comparable intensities, such as $a_i(i = 3\text{–}9)$, $y_i(i = 1\text{–}8)$, G3, G4, and G5. Overall, the spectrum for the peptide G is quite similar to that for the peptide C. At this point, one may be suspicious of the possibility that the spectrum recorded is not due to photodissociation but due to other origins such as CAD induced by gases emitted from instrument surfaces upon high power laser irradiation. Monoisotopic nature of the fragment ions and the fact that the signals disappear when the laser and ion beams are not synchronized are the evidences against such a possibility.

JMS

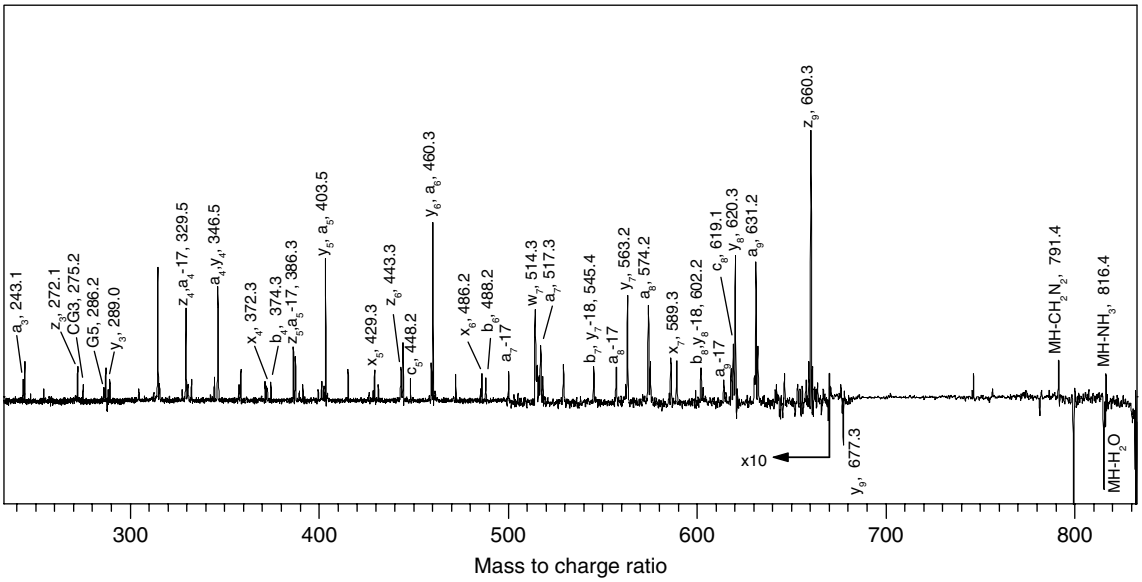

Figure 5. PD spectrum of MH^+ generated by MALDI of the peptide C. 30 mJ PD laser pulse energy resulted in 25% depletion of MH^+.

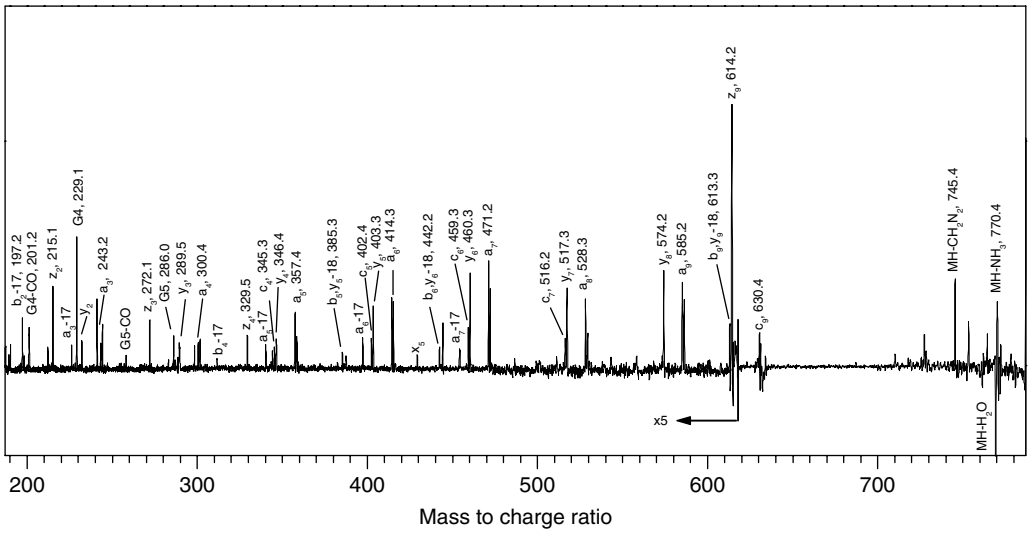

Figure 6. PD spectrum of MH^+ generated by MALDI of the peptide G. 30 mJ PD laser pulse energy resulted in 10% depletion of MH^+.

The PD spectrum for the peptide S, Fig. 7, was recorded with 30 mJ laser pulse energy, which depleted around 25% of the precursor ion. Its main difference from the peptide G spectrum is that the internal acyl peaks are not as prominent as in the latter. Also, unlike in the latter, v_7(515.2) appears distinctly in Fig. 7, which is as expected for a peptide with a seryl residue.

As the final model system, PD spectrum of the peptide H was recorded with 30 mJ laser pulse energy, which depleted around 30% of the precursor ion. Even though the laser energy requirement in this case is similar to that for the peptides without an aromatic residue, the spectral pattern, Fig. 8, resembles those for the peptides with an aromatic residue: in addition to the usual y_8(654.2), a_9(665.3), b_9 or y_9-H_2O(693.4), and z_9(694.2) peaks, a_4-NH_3(363.5), a_4(380.4), y_6(460.3), and v_7(515.1) appear prominently, which are the site-specific peaks in PD of the peptides W, F, and Y.

Angiotensin I

This prototype peptide, DRVYIHPFHL, has one tyrosyl, one phenylalanyl, and two histidyl residues and has been used to test the applicability of the spectral correlations observed in the model systems. Its protonated form could be dissociated efficiently; 3 mJ laser pulse energy resulting in more than 35% depletion. The PD spectrum thus obtained is shown in Fig. 9. Assignments for the major peaks in this spectrum are b_2-NH_3(255.5), y_2(269.4), a_3(343.1), b_3-NH_3(354.2), a_4(506.3), y_4(513.4), b_4-NH_3(517.4), a_5(619.4), b_5(647.3), y_5(650.4), a_6(756.5), b_6(784.6), a_8(1000.6), b_8(1028.7), a_9(1137.6), and z_9(1164.4). These are associated with cleavages near the Y, F, and H residues except for the first two: a_3 and b_3-NH_3 are due to cleavages at the left side of Y, a_4, b_4-NH_3, and b_4 at the right of Y, a_5 and a_6 at the left and right of the first H, respectively, a_8 between F and the second H, and a_9 at the right of the second H. The results are in general

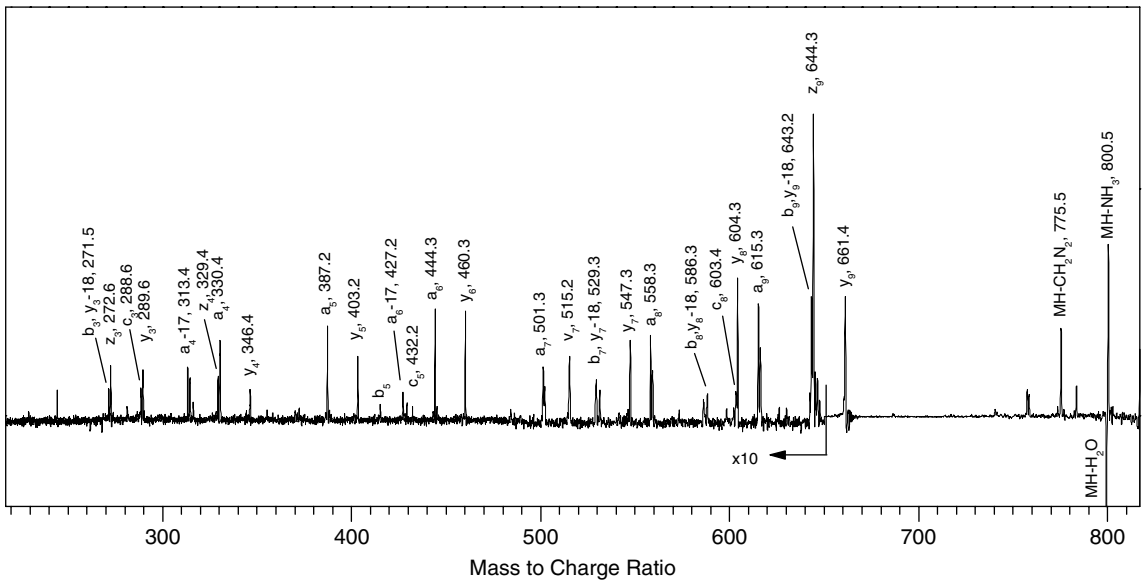

Figure 7. PD spectrum of MH^+ generated by MALDI of the peptide S. 30 mJ PD laser pulse energy resulted in 25% depletion of MH^+.

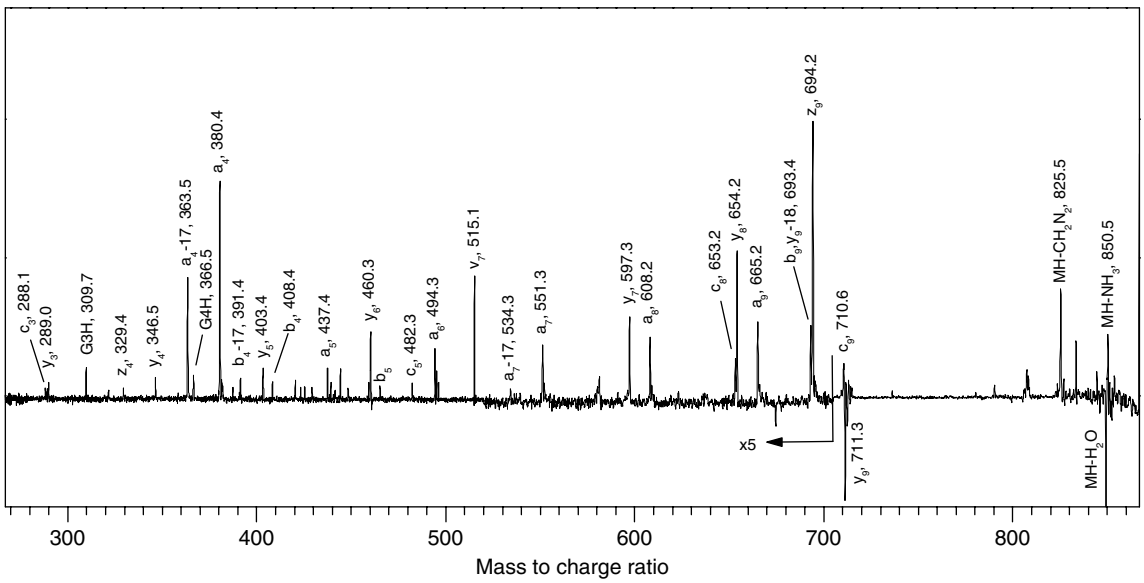

Figure 8. PD spectrum of MH^+ generated by MALDI of the peptide H. 30 mJ PD laser pulse energy resulted in 30% depletion of MH^+.

agreement with the correlation rules even though there are a few exceptions.

DISCUSSION

We have not attempted to determine the relative quantum yield (q) for photodissociation yet, because an accurate measurement requires various difficult experimental arrangements. A very rough estimate can be made via Beer's law treatment of the laser pulse energy (E) used and the precursor ion transmission (T), $q \propto -(\ln T)/E$. Taking the peptide W as the reference, or $q = 1$, the q values for the peptides F, Y, C, G, S, and H thus obtained are 0.3, 0.5, 0.05, 0.02, 0.05, and 0.06, respectively. The large difference in q between the peptides with a tryptophanyl, phenylalanyl, or tyrosyl residue and those without these residues suggests that the photodissociation yield at 266 nm may be useful to distinguish these two groups. From the natural abundances[34] of 1.34, 4.12, and 3.25% for tryptophan, phenylalanine, and tyrosine, respectively, the fraction of peptides without any of these residues can be estimated. For peptides consisting of ten residues, this is around 40% of the total.

Even though the photodissociation quantum yields estimated from the experimental data are only approximate, it is quite evident that these do not correlate well with the molar extinction coefficients quoted previously, even though the latter are the values obtained at 253.7 nm. The most striking are significant photodissociation quantum yields for the peptides G, S, and H. Also surprising is the fact that the photodissociation quantum yield for the peptide

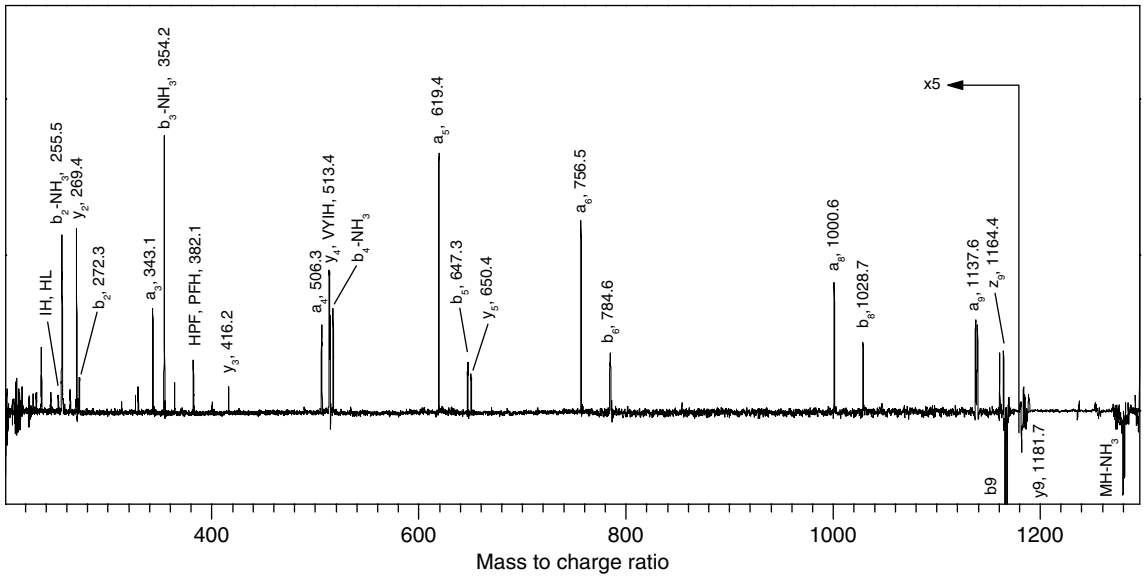

Figure 9. PD spectrum of MH^+ generated by MALDI of angiotensin I. 3 mJ PD laser pulse energy resulted in 40% depletion of MH^+.

C is much less than those for the peptides F and Y even though the extinction coefficients for the three peptides are expected to be comparable. In fact, the peptide C behaves as if it does not contain a significant chromophore. The above data seem to indicate the participation of nonlinear processes such as simultaneous multiphoton absorption in the present PD scheme. A rigorous study is needed for detailed understanding of the processes involved.

It is well known that the sum of the molar extinction coefficients of the amino acid residues constituting a protein or peptide is a good approximation for the same coefficient of the entire molecule.[28] This additivity of absorption suggests that the light energy absorbed, either by one-photon or by multiphoton processes, will be pretty much localized in the chromophore initially and then may dissipate via processes such as internal conversion. If the latter processes are also localized, the result is a vibrationally hot chromophore, or a hot spot in the peptide. Then, the vibrational energy in the hot spot will flow to other parts of the molecules via intramolecular vibrational redistribution (IVR). If dissociation of the peptide bonds connecting the chromophore to the neighboring residues is as fast as or faster than IVR, fragment ions generated by cleavage at these bonds can appear prominently. This is the model we propose for PD of the peptides W, F, and Y. When there is no dominant chromophore, such as in PD at 266 nm of the peptides G and S, photoexcitation is expected to be pretty much delocalized. Then, distribution of the vibrational energy over the entire molecule would result, leading to nonspecific dissociations as observed. In this regard, PD of the peptide H is the case of interest. Here, PD is only as efficient as that of the aliphatic peptides, in agreement with the fact that histidine is not a chromophore at 266 nm. Nevertheless, cleavages near the histidyl residue dominate the PD spectrum. It is not certain whether the results are due to the labile nature of the peptide bonds near the histidyl residue, or the aromatic property of the residue plays some role in the excitation process. We favor the first possibility, even though without any firm evidence.

We have mentioned a few characteristics of PD compared to CAD. The possibility to localize the initial excitation energy, or to generate a hot spot at the chromophore site may be another characteristic of PD. While photoexcitation is a resonance process, collisional activation is not. In addition, CAD for biomolecules is usually practiced under multiple collision condition. Then, the result may be a hot precursor ion with the internal energy distributed over the entire molecule. Nonstatistical reactions are usually difficult to observe in such a case.

CONCLUSIONS

Ion photodissociation in ultraviolet has been generally regarded as a technique that is useful for the fundamental study of ion structure and reaction only. Against this prejudice, we have established that it is a clean and efficient technique which generates a wealth of information on the peptide sequence even when an apparent chromophore is absent. An interesting observation made is that the presence of an aromatic chromophore tends to enhance dissociations in its vicinity while its absence leads to nonspecific dissociations. This can be a useful aspect of the technique in its use as an analytical tool or in the study of peptide chemistry in the gas phase.

Acknowledgements

This work was financially supported by CRI, Ministry of Science and Technology, Republic of Korea. Postdoctoral fellowship to J. H. Moon was supported by CRI. J. Y. Oh thanks the Ministry of Education for the Brain Korea 21 fellowship.

REFERENCES

1. Oh JY, Moon JH, Kim MS. Sequence- and site-specific photodissociation at 266 nm of protonated synthetic polypetides containing a tryptophanyl residue. *Rapid Commun. Mass Spectrom.* 2004; **18**: 2706.
2. Karas M, Bachmann D, Bahr U, Hillenkamp F. Matrix-assisted ultraviolet laser desorption of non-volatile compounds. *Int. J. Mass Spectrom. Ion Processes* 1987; **78**: 53.

3. Tanaka K, Waki H, Ido Y, Akita S, Yoshida Y, Yoshida T. Protein and polymer analyses up to m/z 100 000 by laser ionization time-of-flight mass spectrometry. *Rapid Commun. Mass Spectrom.* 1988; **2**: 151.
4. Kaufmann R, Kirsch D, Spengler B. Sequencing of peptides in a time-of-flight mass spectrometer: evaluation of postsource decay following matrix-assisted laser desorption ionization(MALDI). *Int. J. Mass Spectrom. Ion Processes* 1994; **131**: 355.
5. Kebarle P, Ho Y. On the mechanism of electrospray mass spectrometry. In *Electrospray Ionization Mass Spectrometry*, Cole RB (ed). Wiley: New York 1997; 3.
6. Hop CECA, Bakhtiar R. An introduction to electrospray ionization and matrix assisted laser desorption/ionization mass spectrometry: essential tools in a modern biotechnology environment. *Biospectroscopy* 1997; **3**: 259.
7. Busch KL, Glish GL, McLuckey SA. In *Mass Spectrometry/Mass Spectrometry: Techniques and Applications of Tandem Mass Spectrometry*. VCH Publishers: New York, USA, 1998; 15.
8. Johnson RS, Martin SA, Biemann K. Collision-induced fragmentation of (M + H)+ ions of peptides. Side chain specific sequence ions. *Int. J. Mass Spectrom. Ion processes* 1988; **86**: 137.
9. Morris HR, Paxton T, Dell A, Langhorne J, Berg M, Bordoli RS, Hoyes J, Bateman RH. High sensitivity collisionally-activated decomposition tandem mass spectrometry on a novel quadrupole/orthogonal-acceleration time-of-flight mass spectrometer. *Rapid Commun. Mass Spectrom.* 1996; **10**: 889.
10. Medzihradszhy KF, Campbell JM, Baldwin MA, Falick AM, Juhasz P, Vestal ML, Burlingame AL. The characteristics of peptide collision-induced dissociation using a high-performance MALDI-TOF/TOF tandem mass spectrometer. *Anal. Chem.* 2000; **72**: 552.
11. Loboda AV, Krutchinsky AN, Bromirski M, Ens W, Standing KG. A tandem quadrupole/time-of-flight mass spectrometer with a matrix-assisted laser desorption/ionization source: design and performance. *Rapid Commun. Mass Spectrom.* 2000; **14**: 1047.
12. Cotter RJ. *Time-of-Flight Mass Spectrometry*. American Chemical Society: Washington, DC, 1997; 19.
13. Spengler B. Post-source decay analysis in matrix-assisted laser desorption/ionization mass spectrometry of biomolecules. *J. Mass Spectrom.* 1997; **32**: 1019.
14. Franzen J, Frey R, Holle A, Kräuter K-O. Recent progress in matrix-assisted laser desorption ionization postsource decay. *Int. J. Mass Spectrom.* 2001; **206**: 275.
15. Rinnen KD, Kliner DAV, Blake RS, Zare RN. Construction of a shuttered time-of-flight mass spectrometer for selective ion detection. *Rev. Sci. Instrum.* 1989; **60**: 717.
16. Piyadasa CKG, Håkansson P, Ariyaratne TR, Barofsky DF. A high resolving power ion selector for post source decay measurements in a reflecting time-of-flight mass spectrometer. *Rapid Commun. Mass Spectrom.* 1998; **12**: 1655.
17. Shukla AK, Futrell JH. Tandem mass spectrometry: dissociation of ions by collisional activation. *J. Mass Spectrom.* 2000; **35**: 1069.
18. Jardine DR, Morgan J, Alderdice DS, Derrick PJ. A tandem time-of-flight mass spectrometer. *Org. Mass Spectrom.* 1992; **27**: 1077.
19. Cornish TJ, Cotter RJ. Collision-induced dissociation in a tandem time-of-flight mass spectrometer with two single-stage reflectrons. *Org. Mass Spectrom.* 1993; **28**: 1129.
20. LaiHing K, Cheng PY, Taylor TG, Willey KF, Peschke M, Duncan MA. Photodissociation in a reflectron time-of-flight mass spectrometer: a novel mass spectrometry/mass spectrometry configuration for high-mass systems. *Anal. Chem.* 1989; **61**: 1458.
21. Beussman DJ, Vlasak PR, McLane RD, Seeterlin MA, Enke CG. Tandem reflectron time-of-flight mass spectrometer utilizing photodissociation. *Anal. Chem.* 1995; **67**: 3952.
22. Guan Z, Kelleher NL, O'Connor PB, Aaserud DJ, Little DP, McLafferty FW. 193 nm photodissociation of larger multiply-charged biomolecules. *Int. J. Mass Spectrom. Ion Processes* 1996; **157/158**: 357.
23. Barbacci DC, Russell DH. Sequence and side-chain specific photofragment(193 nm) ions from protonated substance P by matrix-assisted laser desorption ionization time-of-flight mass spectrometry. *J. Am. Soc. Mass Spectrom.* 1999; **10**: 1038.
24. Hettick JM, McCurdy DL, Barbacci DC, Russell DH. Optimization of sample preparation for peptide sequencing by MALDI-TOF photofragment mass spectrometry. *Anal. Chem.* 2001; **73**: 5378.
25. Thompson MS, Cui W, Reilly JP. MALDI photodissociation TOF-TOF mass spectrometry. *Proceedings of the 51st ASMS Conference on Mass Spectrometry and Allied Topics*, Montreal, Canada, 2003.
26. Thompson MS, Cui W, Reilly JP. Fragmentation of singly charged peptide ions by photodissociation at $\lambda = 157$ nm. *Angew. Chem., Int. Ed.* 2004; **43**: 4791.
27. Oh JY, Moon JH, Kim MS. Tandem time-of-flight mass spectrometer for photodissociation of biopolymer ions generated by matrix-assisted laser desorption ionization(MALDI-TOF-PD-TOF) using a linear-plus-quadratic potential reflectron. *J. Am. Soc. Mass Spectrom.* 2004; **15**: 1248.
28. Morton RA. Aminoacids, proteins and enzymes. Fluorescence. *Biochemical Spectroscopy*. John Wiley & Sons: UK, 1975; **1**: 178.
29. Rizzo TR, Park YD, Peteanu LA, Levy DH. The electronic spectrum of the amino acid tryptophan in the gas phase. *J. Chem. Phys.* 1986; **84**: 2534.
30. Martinez III SJ, Alfano JC, Levy DH. The electronic spectroscopy of the amino acids tyrosine and phenylalanine in a supersonic jet. *J. Mol. Spectrosc.* 1992; **156**: 421.
31. Li L, Lubman DM. Analytical jet spectroscopy of tyrosine and its analogs using a pulsed laser desorption volatilization method. *Appl. Spectrosc.* 1988; **42**: 418.
32. Li L, Lubman DM. Ultraviolet-visible absorption spectra of biological molecules in the gas phase using pulsed laser-induced volatilization enhancement in a diode array spectrophotometer. *Anal. Chem.* 1987; **59**: 2538.
33. Biemann K. Contributions of mass spectrometry to peptide and protein structure. *Biomed. Environ. Mass Spectrom.* 1988; **16**: 99.
34. Betts MJ, Russell RB. Amino acid properties and consequences of substitutions. In *Bioinformatics for Geneticists*, Barnes MR, Gray IC (eds). Wiley: West Sussex, 2003; 298.